

Estimation of regional evapotranspiration for a part of WYC command using remote sensing technique

S. K. AMBAST, ASHOK K. KESHARI, A. K. GOSAIN

Department of Civil Engineering (Water Resources Section), I.I.T. Delhi, Hauz Khas, New Delhi 110 016, India

Abstract

Past experience on evapotranspiration has provided sound theoretical knowledge and practical applications that have been validated through field measurements. In spite of its ubiquity, the estimation of evapotranspiration at regional scale in currently used models is based on point source information pertaining to meteorological data. This is mainly due to the difficulty involved in measuring it over a large diverse area or lack of spatial information to estimate it. Remote sensing offers a potential means of measuring outgoing fluxes, surface temperature and leaf area index. In this paper, a remote sensing based methodology is presented to estimate regional evapotranspiration. The methodology is based on surface energy balancing and utilizes the digital data in visible and infrared region alongwith the ancillary meteorological data to derive various fluxes involved in the computation. The developed methodology is utilized to estimate regional evapotranspiration using Landsat-TM data for a part of the Western Yamuna Canal (WYC) command in the State of Haryana, India. Results reveal that the error involved in the estimated average evapotranspiration by the proposed methodology is about 10 % as compared to the estimate obtained by using the Penman-Monteith approach for well-watered crop. The methodology described in this paper is computationally stable, and can be used in practice for most real life applications without sacrificing much accuracy.

INTRODUCTION

The estimation of regional evapotranspiration is of great importance for agricultural, hydrological, atmospheric circulation and climatic change detection models. It constitutes a major part of the hydrological cycle. In spite of its ubiquity, the estimation of evapotranspiration at regional scale in currently used models is based on point information, which represent relatively small area (Daughtry *et al.*, 1990). The conventional ground-based methods for estimating evapotranspiration such as the Bowen ratio (Spittlehouse and Black, 1980), provide accurate measurements over a homogeneous area surrounding the instruments, but it requires an extensive hydrological measurement system over large diverse areas. The one viable means of mapping regional evapotranspiration is remotely sensed spectral data.

Remotely sensed reflectance in visible and infrared regions provides information on surface albedo, surface temperature and vegetation at regional scale. These information along with a few ancillary meteorological data provide the capability of partitioning three of the four surface energy balance components i.e. net radiation, soil heat flux and sensible heat flux. Thus under non-advective conditions, the latent heat flux can be determined

as residual of the surface energy balance. Although recent years have shown the use of some sophisticated models (Kustas *et al.*, 1990; Bastiaanssen, 1995), the degree of complexity varies. These models also require large amount of information that is practically not available in most cases.

The objective of this paper is to demonstrate the application of a model named Regional Evapotranspiration through Surface Energy Partitioning (RESEP), which requires appreciably smaller amounts of ground information and is computationally simple with reasonable accuracy of results (Ambast *et al.*, 2000). The model has been applied to a part of the Western Yamuna Canal (WYC) command in the State of Haryana, India to illustrate the methodology.

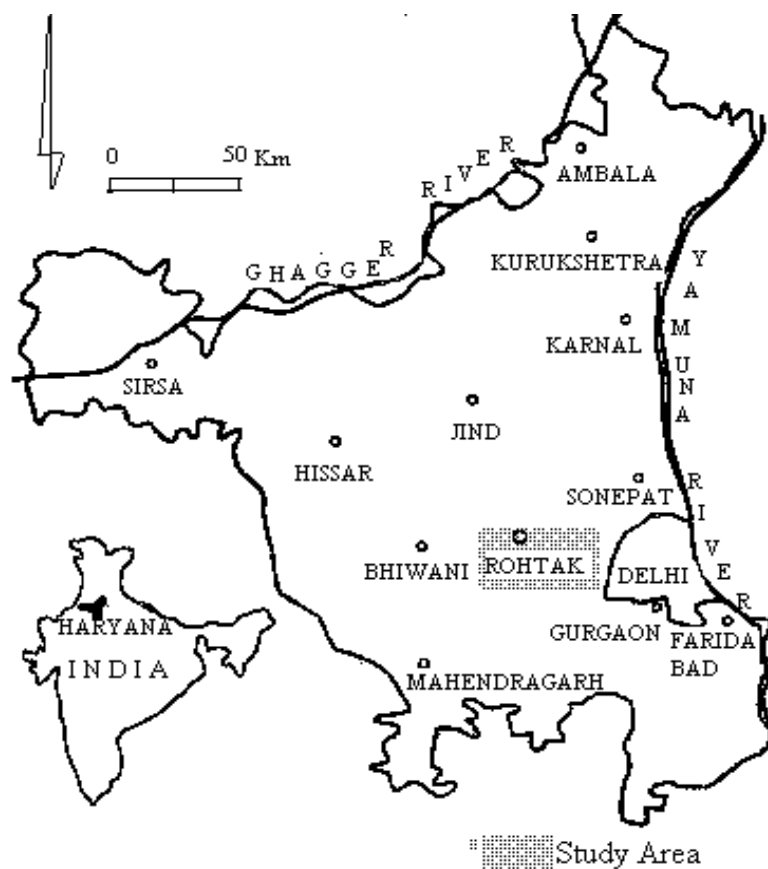


Figure 1. Location map of the study area.

MATERIALS AND METHODOLOGY

Data Used and Study Area

A cloud-free Landsat – TM data (Path/Row-147/040, 30 January 1996) has been analysed for a part of the Western Yamuna Canal system in the State of Haryana, India (Figure 1). The State of Haryana is located in the northern part of India, and falls in arid and

semi-arid region. The area is flat in general, but it forms a topographical depression in the center. The irrigation system during *rabi* (winter) season, when rainfall is almost nil and soil salinity increases to a great extent, is of critical importance. Severe waterlogging exists in the beginning of the crop-growing season, which reduces at the time of crop harvest. However, in many low-lying areas, it remains waterlogged throughout the *rabi* season. Wheat is the major crop during the season and phenologically it attains maximum vegetative growth by middle of February.

Theory

Under negligible advective conditions, latent heat flux (λE , $W m^{-2}$) in surface energy balance equation can be determined as:

$$\lambda E = R_n - G - H \quad (1)$$

where R_n is the net radiation flux ($W m^{-2}$), G is the soil heat flux ($W m^{-2}$) and H is the sensible heat flux ($W m^{-2}$). The energy required for photosynthesis and the heat storage of the plant are comparatively very small, and therefore can be ignored. In equation (1), R_n is considered as positive when radiation is directed towards the land surface, and G , H and λE are considered positive when directed away from land surface.

The net radiation is the algebraic sum of all incoming and outgoing radiation integrated over all wavelengths, expressed as:

$$R_n = R_{s\downarrow} - R_{s\uparrow} + R_{l\downarrow} - R_{l\uparrow} \quad (2)$$

where the subscripts s and l denote shortwave ($0.3-3 \mu m$) and longwave ($3.0-100 \mu m$) radiation ($W m^{-2}$), respectively; and the superscripts \downarrow and \uparrow indicate the incoming and outgoing radiation relative to the earth surface, respectively. The amount of $R_{s\downarrow}$ is a function of time and geographical location of a particular place, whereas $R_{s\uparrow}$ is the radiation reflected by the earth surface. The ratio between $R_{s\downarrow}$ and $R_{s\uparrow}$ is called as surface albedo (ρ_0) and therefore, the net shortwave radiation ($R_{s\downarrow} - R_{s\uparrow}$) is defined as $(1 - \rho_0) R_{s\downarrow}$. The net longwave radiation ($R_{l\downarrow} - R_{l\uparrow}$) is the difference of incoming longwave radiation emitted by the atmosphere and outgoing longwave radiation emitted by the earth surface. It is described by the Stefan-Boltzmann law, and is defined as $(\epsilon' \sigma T_a^4) - (\epsilon_s \sigma T_s^4)$. In this, ϵ' is the apparent atmospheric emissivity (-), σ is the Stefan-Boltzmann constant ($W m^{-2} K^{-4}$), T_a is the air temperature (K), ϵ_s is the grey body emissivity (-) and T_s is the surface temperature (K).

Soil heat flux can not be directly determined through remote sensing techniques. The previous investigations have shown that mid-day G fraction is reasonably predictable from remote sensing determinants of vegetation characteristics, and can be expressed as (Daughtry et al., 1990):

$$G = \Gamma R_n \quad (3)$$

where Γ is the soil heat flux/net radiation fraction (-). Choudhury et al., (1987) introduced a proportionality factor to describe the conductive heat transfer in soil (Γ') and an extinction factor for the attenuation of radiation through canopies (Γ''). Thus, the soil heat flux/net radiation fraction is defined as $\Gamma' \Gamma''$.

The one-dimensional bulk resistance equation for the computation of sensible heat flux is expressed as (Montieth, 1973):

$$H = \rho_a C_p \delta T_{s-a} / r_{ah} \quad (4)$$

where $\rho_a C_p$ is the air heat capacity ($J m^3 K^{-1}$), δT_{s-a} is the surface-air temperature difference (K) and r_{ah} is the aerodynamic resistance to heat transfer ($s m^{-1}$).

The r_{ah} can be estimated as:

$$r_{ah} = \{ \ln((Z_h-d)/Z_{oh}) - \Psi_h \} / (k u^*) \quad (5)$$

where Z_h is the reference height of air temperature and humidity measurements (m), d is the zero plane displacement (m), Z_{oh} is the surface roughness length governing heat and vapour transfer (m), Ψ_h is the stability correction for heat transfer (-), k is the von Karman's constant (-), and u^* is the friction velocity ($m s^{-1}$)

The relationship between wind velocity and friction velocity is given by:

$$u_z / u^* = \{ \ln((Z_m-d)/Z_{om}) - \Psi_m \} / k \quad (6)$$

where Z_m is the reference height of wind measurement (m), Z_{om} is the surface roughness length for momentum transfer (m), u_z is the wind speed measured at height Z_m ($m s^{-1}$), and Ψ_m is the stability correction for momentum transfer (-).

Substituting the value of $1/u^*$ in Eq. (5), the r_{ah} for neutral ($\Psi_h = \Psi_m = 0$, eq.7) and unstable/stable conditions (eq. 8) can be determined as:

$$r_{ah} = \ln((Z_m-d)/Z_{om}) \ln((Z_h-d)/Z_{oh}) / k^2 u_z \quad (7)$$

$$r_{ah} = \{ \ln((Z_m-d)/Z_{om}) - \Psi_m \} \{ \ln((Z_h-d)/Z_{oh}) - \Psi_h \} / k^2 u_z \quad (8)$$

A number of formulations are available for estimating stability corrections. Kustas et al., (1990) used the formulation of Garratt (1978) and Bastiaanssen (1995) used Fiedler and Panofsky (1972) approach for determining the aerodynamic resistance. In the present study, Fiedler and Panofsky's approach is used for estimating stability corrections and thus the distributed aerodynamic resistance of the heat transport.

The roughness length for momentum and heat vary due to the transfer processes of heat and momentum in close proximity of obstacles. A general expression for the relationship between Z_{om} and Z_{oh} is the $Z_{oh} = a Z_{om}$. Although, there has been some efforts to cali-

brate the relationship between Z_{om} and Z_{oh} (Kustas *et al.*, 1989; Brutsaert *et al.*, 1993) at patch scale, the relationship for heterogeneous land surfaces can hardly be obtained in a straight forward manner (Blyth and Dolman, 1995). However, “a” and δT_{s-a} are related because T_s increases with “a” which directly affects δT_{s-a} . On similar grounds, “a” can also be related to u^* (Kustas *et al.*, 1989). Therefore, Dolman and Blyth, (1996) preferred to calibrate δT_{s-a} rather than “a” on account of difficulties to obtain spatial “a” at regional scale. In this study, δT_{s-a} at regional level is calibrated in a different and simplified way, which is discussed in the approach section of this paper.

The actual evapotranspiration (ET_a , $mm\ d^{-1}$) is determined as:

$$ET_a = 8.64 \times 10^7 \Lambda \int_0^{24} (R_n / \lambda \rho_w) \quad (9)$$

where Λ is the evaporative fraction ($\Lambda = \lambda E / (\lambda E + H)$) on instantaneous time basis (-), λ is the latent heat of vapourization ($J\ Kg^{-1}$) and ρ_w is the density of water ($Kg\ m^{-3}$).

Approach

A procedure for determining regional evapotranspiration through surface energy partitioning is developed. It combines analytical and empirical relationships for partitioning of the distributed surface energy balance. Net radiation is obtained from distributed hemispherical surface reflectance and surface radiation temperature data in combination with spatially variable zenith angles for the determination of the clear sky incoming shortwave radiation. The atmospheric corrections are made as applied by Ambast (1997). The flow chart for computation of net radiation is shown in Figure 2.

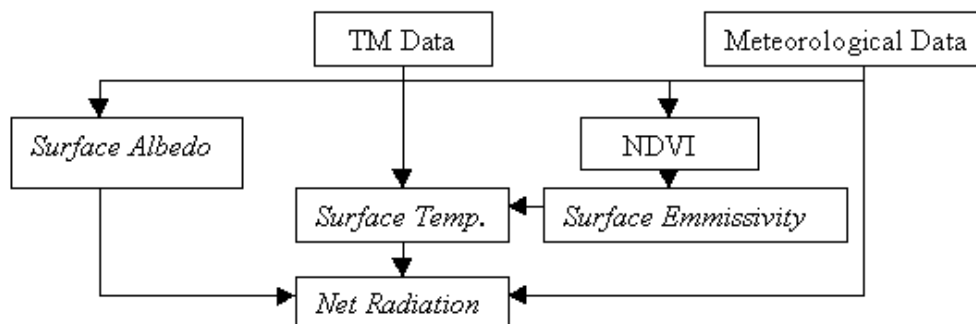


Figure 2. A flow chart for determination of net radiation flux.

An empirical relationship between surface albedo, surface temperature and NDVI, which is used for the same area (Ambast, 1997) is adapted for the computation of soil heat/net radiation flux density fraction and thus soil heat flux. The procedure for determination of soil heat flux is shown in Figure 3.

In order to determine sensible heat flux, a new approach for optimizing δT_{s-a} and thus sensible heat flux is presented in this paper. In this approach, initially distributed aerodynamic resistance for heat is computed assuming neutral stability conditions. The surface-

air temperature difference is obtained by an inversion of the equation for sensible heat transfer for two extreme conditions i.e. where $H = 0$ (wet pixels, $T_{s(\min)}$) and one where $\lambda E = 0$ (dry pixel, $T_{s(\max)}$) and coupled linearly with T_s . The linear relationship between T_s and T_a at 1.5 m is well reported by Horiguchi *et al.*, (1992). Uncorrected sensible heat flux is determined using aerodynamic resistance and surface-air temperature difference under neutral stability condition.

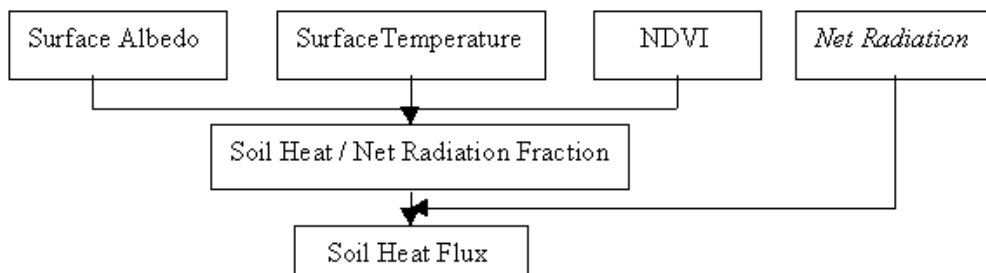


Figure 3. A flow chart for determination of soil heat flux.

To compute uncorrected sensible heat flux, a relationship between NDVI and LAI for wheat crop (Dellán, 1997) predominant in the study area is used to generate the LAI image. Calculated LAI are compared with LAI measured by a hand held LAI meter (LICOR-2000) in the study area, which are found in good agreement ($r^2=0.92$) (Ambast, 1997). The height d and Z_{om} in aerodynamic resistance equations are the functions of crop height (h_c) and roughness, and vary according to canopy structure. Distributed crop height is obtained by a relationship between crop height and leaf area index representative for actual growing conditions in the study area (Kumar, 1981). A general approximation based on experimental and theoretical considerations proposed by Perrier (1982) for crops with LAI more than 0.5 has been used in the present study for determining distributed d and Z_{om} . Since, the momentum transfer governs the heat and vapour transfer, the roughness height for heat transfer is assumed to be a fraction of roughness height for momentum ($Z_{oh}=a Z_{om}$). The value of “a” is taken as 0.1 as suggested for fully covering crops (Monteith 1973).

For improving the aerodynamic resistance values, the average stability correction factor for the region is determined as average of stability correction factor for driest pixel and wettest pixel. For determining stability correction factor for driest pixel, initial Ψ_m is taken as zero and u_z at 2 m is taken as 2.5 Km/hr from a nearby meteorological observatory. Iterations are made to arrive at the converged value of stability correction on the basis of air temperature difference for two successive iterations to be less than 0.1. The average stability correction value is used to generate distributed values of friction velocity, Monin-Obhukhov length and stability correction for heat and momentum. These values are assigned in successive iterations to improve the distributed aerodynamic resistance for heat and optimizing the surface-air temperature difference. The improved distributed aerodynamic resistance for heat and surface-air temperature difference is used in one dimensional bulk resistance equation (Eq. 4) to generate the improved distributed sensible heat flux. For convergence, the air temperature difference of pixel having maxi-

mum surface temperature for successive iteration less than 0.1 is taken as criteria. A flow chart illustrating the methodology to compute the sensible heat flux is shown in Figure 4.

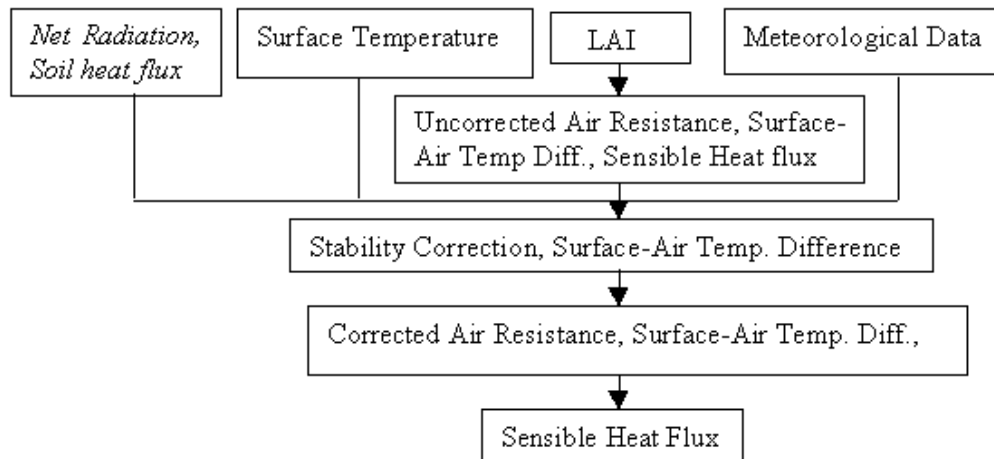


Figure 4. A flow chart for determination of sensible heat flux.

After knowing all components of the surface energy balance, latent heat flux density is finally obtained as the residue of the land surface energy balance. The regional evapotranspiration (mm d^{-1}) is then determined using evaporative fraction on instantaneous time basis with total energy integrated over the day.

RESULTS AND DISCUSSION

Operationally, the RESEP first generates surface albedo (r_o), surface temperature (T_s), normalized difference vegetation index (NDVI), and leaf area index (LAI) images using the digital data in the visible and infrared regions. In continuation of generating above images, it computes the components of radiation i.e. incoming and outgoing shortwave radiation and incoming and outgoing longwave radiation to yield net radiation flux (R_n). The incoming shortwave and longwave radiations are calculated as 494 W m^{-2} and 354 W m^{-2} , respectively on the date of satellite pass for the study area. The R_n image (W m^{-2}) is shown in Figure 5(a). The statistical analysis indicates the R_n values between $175\text{--}500 \text{ W m}^{-2}$ and the mean value as 406 W m^{-2} . For cropped areas, the R_n values are observed between $380\text{--}440 \text{ W m}^{-2}$. The water bodies are having higher R_n values ($440\text{--}500 \text{ W m}^{-2}$), whereas for dry areas it is observed lower values ($200\text{--}380 \text{ W m}^{-2}$) than the cropped areas.

The determination of soil heat flux (G) is the next step in the proposed RESEP model. The G image (W m^{-2}) is shown in Figure 5(b). It is ranging between $20\text{--}70 \text{ W m}^{-2}$ and the mean G is calculated as 43 W m^{-2} . For cropped areas, the G value is observed between $35\text{--}50 \text{ W m}^{-2}$. The water bodies is having lower G value ($<35 \text{ W m}^{-2}$), whereas for non-cropped dry areas it is observed higher ($50\text{--}70 \text{ W m}^{-2}$) than the cropped areas.

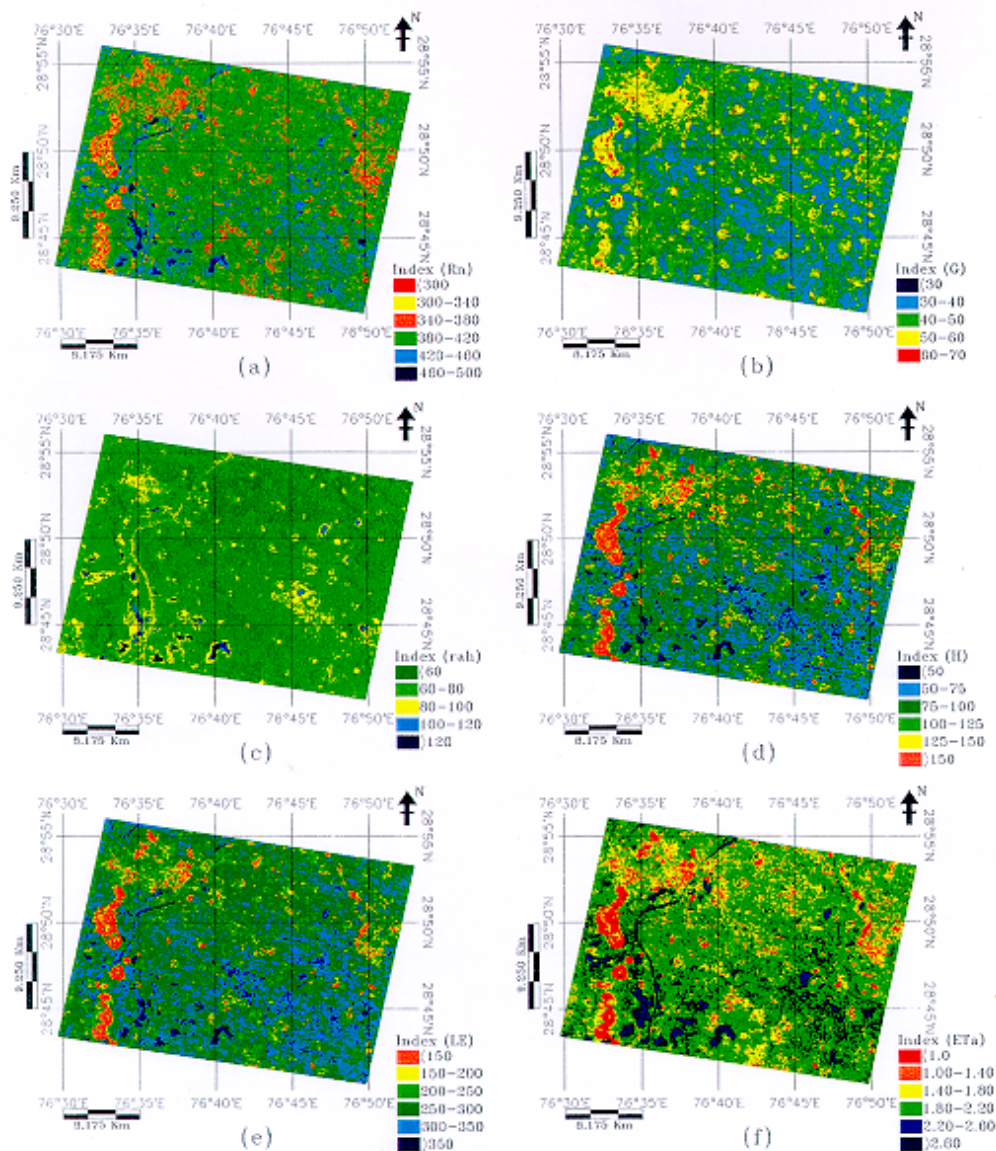


Figure 5. Images showing (a) net radiation flux (b) soil heat flux (c) aerodynamic resistance for heat (d) sensible heat flux (e) latent heat flux and (f) actual evapotranspiration for a part of the WYC command.

The determination of sensible heat flux (H) requires much more attention due to its strong dependence on local meteorological conditions. In the proposed methodology, initially an uncorrected version of aerodynamic resistance for heat (r_{ah}) values are obtained. For highest temperature pixel ($T_{s(max)}$), the extracted r_{ah} value is observed 277.51 m^{-1} , but this resulted in a negative air temperature showing unstable condition. An itera-

tive procedure is made, and the optimum value of stability correction for momentum (Ψ_m) for $T_{s(\max)}$ pixel is obtained as 1.96. Since wet pixels (water bodies) are having Ψ_m equal to 0, $\Psi_{m(\text{avg})}$ is taken as 0.98 and assigned as initial value of Ψ_m for whole sub-scene. The iterative procedure is used to obtain the distributed values of u^* , L , Ψ_m and Ψ_h . For the given convergence criteria ($T_{a(i-1)} - T_{a(i)} < 0.1$ for $T_{s(\max)}$), an improved value of r_{ah} as 74.6 s m^{-1} is obtained after two iterations. The image for improved r_{ah} is shown in Figure 5(c). The low r_{ah} values ($< 40 \text{ s m}^{-1}$) are observed for smooth cropped areas, whereas high values ($> 80 \text{ s m}^{-1}$) are observed for built-up areas and water bodies. The statistical analysis indicates that the of surface-air temperature difference (δT) range between $0\text{-}14 \text{ }^\circ\text{C}$. For water bodies and cropped areas with high water availability, δT is observed less than $4 \text{ }^\circ\text{C}$, whereas for cropped areas with average or less water availability, it is in between $4\text{-}8 \text{ }^\circ\text{C}$ (Figure not shown). For dry non-cropped areas, δT is observed more than $10 \text{ }^\circ\text{C}$. The H image (W m^{-2}) is shown in Figure 5(d). Statistical analysis indicates the range of H between $0\text{-}300 \text{ W m}^{-2}$. For cropped areas, the H is observed between $50\text{-}150 \text{ W m}^{-2}$. The water bodies are having H values less than 50 W m^{-2} , whereas for dry non-cropped areas H is observed more than 150 W m^{-2} .

For the sub-scene, the latent heat flux (λE) is observed between $0\text{-}425 \text{ W m}^{-2}$ (Figure 5(e)). The mean λE is calculated to be 270 W m^{-2} . Although the λE and H images are identical in appearance, the index values are just reverse. This shows that the pixels having low H value are having high λE value and vice-versa. Further, the evaporative fraction (Λ) image is generated and used for estimating the actual evapotranspiration (ET_a) image. The statistical analysis indicates the range of ET_a between $0\text{-}3.0 \text{ mm d}^{-1}$ and the mean value is calculated as 1.9 mm d^{-1} . For cropped areas, ET_a is observed between $1.8\text{-}2.2 \text{ mm d}^{-1}$ (Figure 5f). The water bodies evaporate water at potential and is observed more than 2.2 mm d^{-1} . For dry areas, evaporation is observed less than 0.5 mm d^{-1} .

In absence of ground information on energy fluxes, in the present study the validation is made by comparing the estimated ET_a by the proposed model with the one obtained by Penman-Monteith equation using the meteorological data for wheat crop. For well-watered crop (NDVI and $\Lambda > 0.8$), the average ET_a by proposed model is observed 2.1 mm d^{-1} ; whereas using Penman-Monteith equation, it is calculated as 1.9 mm d^{-1} . Though the model is over estimating the actual evapotranspiration, but is still close to the error margin of 10%.

CONCLUSIONS

Conventional methods of estimating the distributed actual evapotranspiration over a large area require an extensive hydrological measurement system. Remote sensing offers a means of measuring outgoing fluxes and vegetation at regional scale. The results reported here indicate that a satellite based operational technique will yield components of surface energy balance on instantaneous time basis, and can be used for generating the daily evapotranspiration at regional scale. The proposed model utilizes a simplified approach for estimating the aerodynamic resistance and optimizing surface-air temperature difference, and thus enables us to make it operational. The distributed values of actual

evapotranspiration obtained from the proposed RESEP model can be utilized in the distributed hydrological models for improving the hydrological simulations.

References

- Ambast, S. K. (1997), "Monitoring and evaluation irrigation system performance in saline irrigated command through SRS and GIS", Report No. 471, DLO-Winand Staring Centre, Wageningen, The Netherlands.
- Ambast, S. K., Keshari, A. K. and Gosain, A. K. (2000), "Regional evapotranspiration through surface energy partitioning using satellite remote sensing", Paper communicated to Remote Sensing of Environment.
- Bastiaanssen, W. G. M. (1995), "Regionalization of surface fluxes and moisture indicators at composite terrain", Ph.D. Thesis, Wageningen Agricultural University, Wageningen, The Netherlands.
- Blyth, E. M. and Dolman, A. J. (1995), "The roughness length for heat of sparse vegetation", *Journal of Applied Meteorology*, 34:583-585.
- Brutsaert, W. H., Hsu, A. Y. and Schmugge, T. J. (1993), "Parameterization of surface heat fluxes above forest with satellite thermal sensing and boundary layer soundings", *Journal of Applied Meteorology*, 32:909-917.
- Choudhury, B. J., Idso, S. B. and Reginato, R. J. (1987), "Analysis of an empirical model for soil heat flux under a growing wheat crop for estimating evaporation by an infrared temperature based energy balance equation", *Agricultural Forest Meteorology*, 39: 283-297.
- Daughtry, C. S. T., Kustas, W. P., Moran, M. S., Pinter, P. J. Jr., Jackson, R. D., Brown, P. W., Nichols, W. D. and Gay, L.W. (1990), "Spectral estimates of net radiation and soil heat flux", *Remote Sensing of Environment*, 32:111-124.
- Dellan, A. (1997), Unpublished M.Sc. Thesis, Wageningen Agricultural University, The Netherlands.
- Dolman, A. J. and Blyth, E. M. (1996), "Patch scale aggregation of heterogeneous land surface cover for mesoscale meteorological models", *Journal of Hydrology (Special Issue)*, Tuckson.
- Fiedler, F. and Panofsky, H. A. (1972), "The geostrophic drag coefficient and the effective roughness length", *Quarterly Journal of Royal Meteorological Society*, 98:213-220.
- Garratt, J. R. (1978), "Transfer characteristics for a heterogeneous surface of large aerodynamic roughness", *Quarterly Journal of Royal Meteorological Society*, 104: 491-502.
- Horiguchi, I., Tani, H. and Motoki, T. (1992), "Accurate estimation of 1.5 m height air temperature by GMS-IR data", *Proceedings 24th International Symposium on Remote Sensing of Environment*, Rio de Janeiro, pp. 301-307.
- Kumar, Ashok (1981), "Growth and yield behaviour of wheat varieties under dry and wet soil moisture environment", M. Sc. Thesis. Department of Agronomy, C.C.S. Haryana Agricultural University, Hisar, India.
- Kustas, W. P., Choudhury, B. J., Moran, M. S., Reginato, R. J., Jackson, R. D. Gay, L.W., Weaver, H. L. (1989), "Determination of sensible heat flux over sparse canopy using thermal infrared data", *Agricultural Forest Meteorology*, 44, 197-216.
- Kustas, W. P., Moran, M. S., Jackson, R. D., Gay, L.W., Duell, L. F. W., Kunkel, K. E. and Matthias, A. D. (1990), "Instantaneous and daily values of the surface energy balance over agricultural fields using remote sensing and a reference field in an arid environment", *Remote Sensing of Environment*, 32:125-141.
- Monteith, J. L. (1973), "Principles of Environmental Physics", Edward Arnold, London.
- Perrier, A., (1982), "Land surface processes: vegetation", *Proceedings on Land Surface Processes in Atmospheric General Circulation Model*, Cambridge University Press, Cambridge, pp. 395-448.
- Spittlehouse, D. L. and Black, T. A. (1980), "Evaluation of the Bowen ratio/energy balance method for determining forest evapotranspiration", *Atmosphere-Ocean*, 18:98-116.